n-Butane isomerization over $SO_4^{=}/NiO/Al_2O_3/ZrO_2$ catalysts. Effect of the reaction pressure and metal loading

M. Perez-Luna [a,b], J.A. Toledo-Antonio [a,*], F. Hernandez-Beltrán [a], H. Armendariz [a] and A. García Borquez [c]

[a] *Instituto Mexicano del Petróleo, Prog. Ing. Molecular, L. Cárdenas No. 152, 07730 México, D.F. México*
[b] *Instituto Politécnico Nacional, ESIQIE. Edif. No. 8 U. Prof. A. López Mateos, Zacatenco, 07730 México, D.F. México*
[c] *Instituto Politécnico Nacional, ESFM. Edif. No. 9 U. Prof. A. López Mateos, Zacatenco, 07730 México, D.F. México*

Received 14 February 2002; accepted 28 June 2002

The effect of alumina and nickel in sulfated ZrO_2 as a catalyst for *n*-butane isomerization was investigated. Samples were synthesized by supporting nickel sulfated zirconia on boehmite and then calcining the material. The crystalline structure of ZrO_2 was studied by X-ray powder diffraction and refined by the Rietveld method. Surface areas were determined by N_2 adsorption and BET analysis, while the acid properties were studied by NH_3 adsorption. The chemical reaction was carried out in a fixed-bed microreactor at 338 K under atmospheric (78 kPa) or 245 kPa total pressure. Results showed that either nickel or alumina improved the catalytic activity, but a synergic effect was observed when both components assisted. The catalytic activity was related to the relative content of tetragonal zirconia and acid site density. Alumina stabilized tetragonal zirconia increased the acid site density and presumably led to a better dispersion of nickel oxide. The catalytic activity could be related to both oxidation and acid sites produced by nickel. A bimolecular reaction mechanism helps explain the observed trends. The increase in the reaction rate would be explained by the increase in the rate of the initial step of dehydrogenation either caused by a better dispersion of nickel or higher operating pressure.

KEY WORDS: sulfated zirconia; nickel–alumina-promoted sulfated zirconia; mixed oxides; *n*-butane isomerization; tetragonal and monoclinic zirconia.

1. Introduction

In general, the oil-refining industry faces serious constraints imposed by clean-fuel programs worldwide. Stringent regulations on gasoline in the USA and Europe limiting the percentage of sulfur, olefins, total aromatics, benzene, vapor pressure and distillation endpoint affect the demand and quality for every major gasoline-blend component, *i.e.*, FCC naphtha, reformate, etc. The alkylation of light hydrocarbons produces an extremely valuable gasoline-blending component that overcomes all those constraints. Therefore, it clearly appears that alkylation is a key reaction supporting reformulated gasoline strategies because of the high octane and paraffinic and contaminant-free nature of the gasoline that is produced. The growing demand for alkylate implies that the demand for iso-butane and iso-butene in a refinery will certainly keep going up in the near future.

The main source of iso-butane in a refinery is the fluid catalytic cracking process. However, the amount of iso-butane that this process can provide is relatively limited in part because of the constraints imposed by thermodynamics limiting the relative amount of i-C_4 to total butanes. The isomerization of *n*-butane could be an alternative to increase the availability of iso-butane [1]. Catalysts based on zirconia (ZrO_2) modified with sulfate ions have been shown to be more active for this reaction than conventional chlorided alumina or zeolites [2]. In spite of the apparent simplicity for preparing sulfated ZrO_2, there are a number of key issues that can seriously modify the catalytic properties, *i.e.*, synthesis of zirconium hydroxide, the sulfation process, thermal treatment, etc. The addition of Ni (and other transition metals, such as Fe and Mn) to sulfated zirconia is known to improve the catalytic activity and stability for isomerization reactions [3–5]. These metals lead the isomerization pathway to shift from a monomolecular to a bimolecular mechanism. According to the latter mechanism, the butane molecule reacts with an adsorbed carbenium ion [6–8].

On the other hand, it has been reported that supporting ZrO_2 in γ-alumina improved the catalytic activity for *n*-butane isomerization [9]. This was explained in terms of increasing ZrO_2 dispersion and the density of Lewis acid sites.

In view of the growing interest in the alkylation reaction and the potential of ZrO_2 as an isomerization catalyst, we were prompted to study the effect of distinct variables in the catalytic activity of sulfated ZrO_2 for *n*-butane isomerization. We studied the effect of γ-alumina, Ni and the sulfate content related to the crystalline phases and the acid properties of ZrO_2. Samples were evaluated for *n*-butane isomerization at 78 kPa and 245 kPa pressure.

* To whom correspondence should be addressed.
E-mail: Jtoledo@imp.mx

1011-372X/02/1100-0201/0

2. Experimental

2.1. Synthesis of materials

The synthesis of sulfated ZrO_2 samples used in this work was based on a method reported elsewhere [10]. Briefly, an aqueous solution (28 vol%) of ammonium hydroxide (J.T. Baker) was added dropwise to a solution of $ZrO(NO_3)_2$ (Aldrich, 99%) at room temperature until a pH of 9.5 was reached. The $Zr(OH)_4$ formed as a precipitate was filtered, washed thoroughly with deionized water and dried at 373 K overnight. The dry solid was powdered and divided into six portions. The sample coded ZS-12.0 was produced by sulfating by the incipient-wetness method using a solution of H_2SO_4 (J.T. Baker, 96 vol%). Five samples were produced similarly, except that the H_2SO_4 solution contained a controlled amount of $Ni(NO)_3$ $6H_2O$ (Aldrich, 99%). The amount of nickel nitrate and the volume of sulfuric acid used supplied 0.8 wt% NiO and 10–13 wt% $SO_4^{=}$ respectively in the final solids. Samples were dried at 373 K overnight and, finally, they were manually extruded to $\frac{1}{8}$in. cylindrical particles with peptized ($\frac{1}{32}$vol/vol HNO_3 water) boehmite (Catalpal, Vista) and calcined at 948 K for 1 h in flowing air. Samples were coded as ZANS-X, where X indicates the wt% sulfate, A stands for alumina and N for nickel.

2.2. Characterization techniques

The chemical composition was determined by Atomic Absorption Spectroscopy in a Perkin Elmer S-2380 apparatus. The sulfur content was determined by combustion in a LECO SC-44 apparatus.

Specific-surface-area measurements were carried out in a Micromeritics Digisorb 2600 apparatus according to ASTM-D-3663.

X-ray diffraction patterns of powdered samples were recorded at room temperature with a Cu K_α radiation Siemens D500 diffractometer having theta–theta configuration and a graphite secondary-beam monochromator. The diffraction pattern was recorded in the 2θ range between 10 and 70°. Crystalline structures were refined with the Rietveld technique by using FULLPROF-V3.5d [11] codes. This technique led to determining crystallite size, cell parameters and the relative content of crystalline phases of ZrO_2.

The total acidity was measured by NH_3 titration in an Altamira AMI 2000 equipped with a thermal conductivity detector (TCD). 200 mg of sample were pretreated under flowing N_2 at 773 K for 4 h. Then, the sample was cooled down to 423 K. Calibrated pulses of NH_3 were injected through a six-port on-line valve until saturation of the sample was reached. The amount of NH_3 adsorbed by the sample was calculated from the difference between total NH_3 injected and the amount of NH_3 calculated from the TCD signals.

2.3. Catalytic activity

The catalytic activity of solids was studied in the isomerization of *n*-butane. The reaction was carried out in a flowing-system stainless-steel fixed-bed microreactor (7 mm diameter, 150 mm length) using 0.5 g powdered sample previously treated under air (30 cm^3/min) at 773 K for 1 h. A flow of 2.5 cm^3/min of *n*-butane (Matheson C.P.) was fed to the reactor while the temperature was previously fixed at 338 K. The reaction was carried out either at atmospheric (78 kPa) or 245 kPa total pressure. The reaction products were analyzed on-line in a Hewlett-Packard 5890 Gas Chromatograph equipped with a 3 m × $\frac{1}{8}$in. packed column (Porasil C) and TCD.

3. Results

3.1. Textural, structural and acid properties

The properties of samples are presented in table 1. Due to the preparation method, the Ni and alumina contents in the catalysts were quite reproducible. The sulfate content ranged from 10.7 to 13.4 wt%.

Alumina increased the catalyst surface area about 28% (table 1) compared to sulfated zirconia alone. All the alumina-supported samples showed very similar values of specific surface area ranging between 109 and

Table 1
Chemical composition, textural and acidic properties of the zirconia samples.

Sample	Chemical composition (wt%)				Specific area (m^2/g)	Porous volume (cm^3/g)	Mean porous size (Å)	Acid site density (meq NH_3/m^2)
	ZrO_2	NiO	Al_2O_3	$SO_4^{=}$				
ZS-12.0	100	0.0	0.0	12.0	92	–	–	3.4
ZAS-10.7	78.2	0.0	11.1	10.7	118	0.10	42.6	2.7
ZANS-10.7	77.3	0.8	11.1	10.7	116	0.13	46.8	8.1
ZANS-11.6	76.4	0.8	11.1	11.6	109	0.11	40.9	10.4
ZANS-12.5	75.5	0.8	11.1	12.5	110	0.15	55.7	9.3
ZANS-13.4	74.6	0.8	11.1	13.4	112	0.15	42.6	8.8

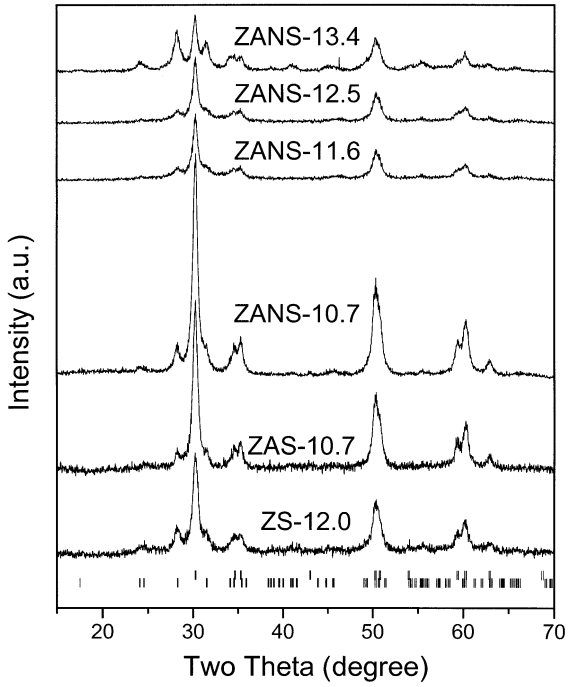

Figure 1. X-Ray diffraction patterns of the sulfated zirconia–alumina samples. Upper tick marks correspond to the tetragonal zirconia phase and the lower ones the monoclinic zirconia phase.

$118\,m^2/g$. It was found that nickel had no major effect on the textural properties except for some increase in pore volume from 0.10 to $0.13\,cm^3/g$. Similarly, a slight increase in pore volume apparently related to the sulfate content was also observed.

The acid site density in terms of the specific surface (table 1) was calculated from the NH_3 adsorption data. Compared to sulfated ZrO_2 alone, the acid site density showed no change when the material was supported on alumina. However, when nickel and aluminum were both associated (samples ZANS-X), the acid site density strongly increased. In a previous paper [10], we reported that nickel had not affected the acid site density in sulfated ZrO_2. Therefore, it seems that nickel and aluminum are both required for promoting the acid properties in sulfated ZrO_2.

Figure 1 shows the X-Ray diffraction pattern of samples. All the samples showed tetragonal and monoclinic phases of ZrO_2 in somehow different proportions. No evidence of either the NiO or γ-Al_2O_3 phase was found in samples ZANS-X, which was attributed to the lower content of nickel and the microcrystalline nature of γ-Al_2O_3.

Tetragonal ZrO_2 was modeled using a unit cell symmetry described by the space group $P4_2/nmc$ and the atomic positions reported elsewhere [12], while monoclinic ZrO_2 was modeled with a unit cell that had a $P2_1/c$ space group symmetry [13]. Table 2 summarizes the relative content of crystalline phases and the crystallite size and lattice parameters obtained from Rietveld analysis.

Table 2
Structural parameters of the tetragonal and monoclinic zirconia phases.

Sample	Phase	Phase conc. (wt%)	Crystallite size (Å)	Lattice parameters (Å)		
				a	b	c
ZS-12.0	Tetragonal	63	145	3.598	3.598	5.183
	Monoclinic	37	120	5.136	5.196	5.327
ZAS-10.7	Tetragonal	90	159	3.594	3.594	5.183
	Monoclinic	10	190	5.147	5.182	5.313
ZANS-10.7	Tetragonal	76	158	3.591	3.591	5.178
	Monoclinic	24	114	5.135	5.195	5.317
ZANS-11.6	Tetragonal	78	95	3.599	3.599	5.178
	Monoclinic	22	178	5.118	5.198	5.329
ZANS-12.5	Tetragonal	75	102	3.594	3.594	5.175
	Monoclinic	25	170	5.116	5.195	5.329
ZANS-13.4	Tetragonal	27	164	3.598	3.598	5.182
	Monoclinic	73	85	5.135	5.206	5.326

It was observed that γ-Al_2O_3 stabilizes the tetragonal phase of ZrO_2. The relative content of the tetragonal phase of ZrO_2 increased from 63 wt% ZS-12.0 up to *ca* 90 wt% in ZAS-10.7. However, it decreased to 76 wt% upon nickel addition. This could be explained by assuming that some Ni atoms reacted with alumina, thus forming nickel aluminate, not detected by XRD patterns due to its low concentration. Therefore, upon nickel addition lower amounts of aluminum were available for interaction with zirconia.

The relative content of tetragonal ZrO_2 remained constant between 10.7 and 12.5 wt% sulfate. Increasing sulfate content up to 13 wt% caused the relative content of tetragonal ZrO_2 to decrease dramatically, and thus larger amounts of monoclinic phase were obtained.

The average crystallite size of tetragonal ZrO_2 showed no major change with Ni and Al_2O_3 (table 2). However, when the sulfate content increased, the crystallite size decreased from *ca* 150 Å to *ca* 100 Å, then increased again up to 164 Å for the highest sulfate content and the lowest relative content of tetragonal ZrO_2, sample ZANS-13.4. It seems, therefore, that the optimum sulfate content in our samples was slightly lower than 13 wt%. These results are in agreement with that reported by Farcasiu *et al.* [14], who found a sulfate concentration of 15 wt% as the optimum value to stabilize tetragonal ZrO_2.

3.2. Catalytic activity

3.2.1. n-Butane isomerization at atmospheric pressure

Figure 2 shows *n*-butane conversion data collected at atmospheric pressure (78 kPa) as a function of time on stream (tos). Sulfated ZrO_2 showed very poor catalytic activity. Conversion was under 1 mol%. The catalytic activity improved with alumina-supported ZrO_2, showing *n*-butane conversion up to 5 mol%. The highest

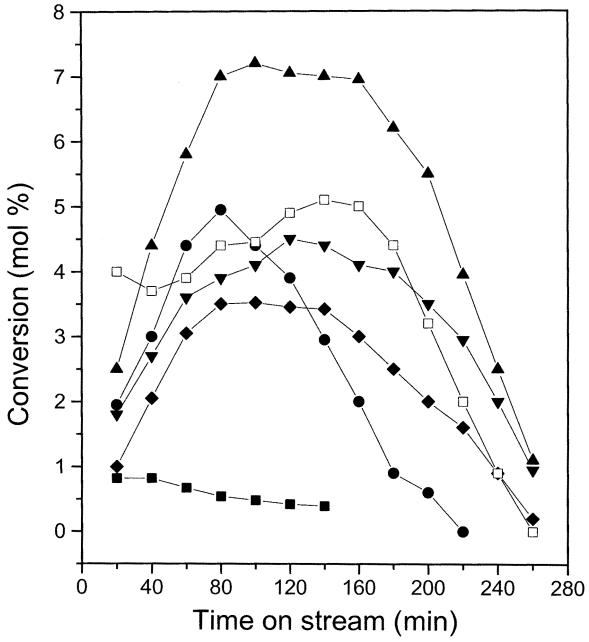

Figure 2. Conversion *versus* time on stream in *n*-butane isomerization at atmospheric pressure (78 kPa). (■) ZS-12.0; (●) ZAS-10.7; (▲) ZANS-10.7; (▼) ZANS-11.6; (◆) ZANS-12.5; (□) ZANS-13.4.

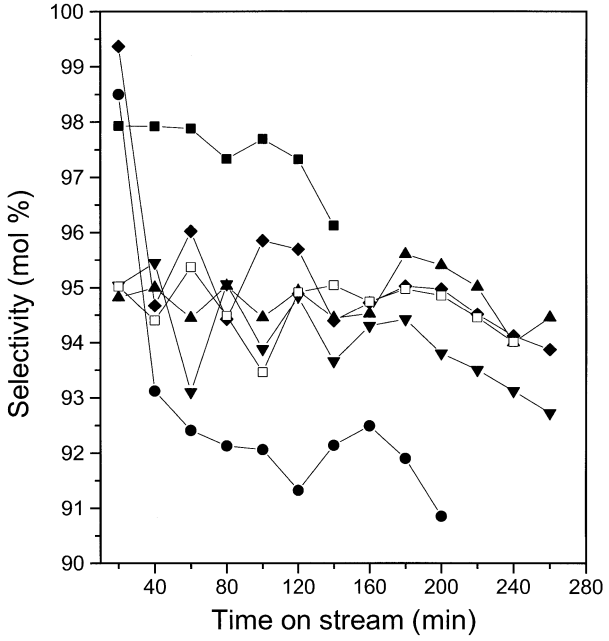

Figure 3. Selectivity to isobutane *versus* time on stream in *n*-butane isomerization reaction at atmospheric pressure (78 kPa). (■) ZS-12.0; (●) ZAS-10.7; (▲) ZANS-10.7; (▼) ZANS-11.6; (◆) ZANS-12.5; (□) ZANS-13.4.

catalytic activity was observed with nickel–alumina samples. However, these solids showed an induction period at the earliest stages of the reaction showing a maximum between 80 and 160 min tos, then deactivation proceeded. Other authors have reported similar trends and induction periods on sulfated zirconia promoted with metals [15–17]. This induction period has been related to the formation of dehydrogenated species on the catalyst surface according to the hypothesis of a bimolecular mechanism [8]. Although alumina increased the activity of sulfated ZrO_2 the stability was very poor (figure 2 and table 3). Nickel was shown to improve activity and stability over larger periods of tos. On the contrary, sulfate content over 13 wt% seemed to reduce the catalytic activity and stability.

Table 3
Intrinsic activity of the zirconia samples during *n*-butane isomerization reaction.

Sample	Intrinsic activity atmospheric pressure $(mol/s\,m^2) \times 10^8$			Intrinsic activity 2.5 kg/cm^2 pressure $(mol/s\,m^2) \times 10^7$		
	60 min	200 min	Stability	60 min	200 min	Stability
ZS-12.0	0.31	0.00	0.00	–	–	–
ZAS-10.7	1.56	0.21	0.14	1.15	0.84	0.73
ZANS-10.7	2.10	1.99	0.95	3.38	2.83	0.84
ZANS-11.6	1.39	1.35	0.94	2.67	1.26	0.47
ZANS-12.5	1.16	0.76	0.65	3.01	2.19	0.71
ZANS-13.4	1.46	1.20	0.82	0.72	0.39	0.53

The main reaction product observed was iso-butane with small amounts of propane and iso-pentane. No major changes in iso-butane selectivity due to changes in catalytic activity were observed. Iso-butane selectivity ranged between 93 and 96% for all materials except ZAS-10.7. This sample showed a selectivity of *ca* 98%, which decreased somehow at the test front-end (figure 3).

3.2.2. *n-Butane isomerization at 245 kPa of pressure*

Compared to previous runs the *n*-butane conversion strongly improved when the reaction was carried out at 245 kPa of total pressure. Conversion data plotted in figure 4 as a function of tos show that a conversion level under 10 mol% was observed with sample ZANS-13.4. The absence of Ni in sample ZAS-10.7 seemed also to decrease the activity of the catalyst when compared to the Ni-alumina materials. The initial conversion increased up to 50 mol% and 40 mol% for samples ZANS-10.7 and ZANS-11.6, but deactivation was quite pronounced. The catalytic activity dropped to 80% after 200 min tos. Sample ZANS-12.5 showed a similar induction period previously observed at atmospheric pressure (78 kPa). The maximal conversion was 28 mol%, while the deactivation trend after this induction period was similar to the other samples.

Iso-butane selectivity ranged between 90 and 95% for all samples and tends to decrease with deactivation (figure 5). Secondary products were also propane and pentanes, thus suggesting that the same reaction mechanism operates as at atmospheric pressure. However, in this case a very fast deactivation was observed. It is possible

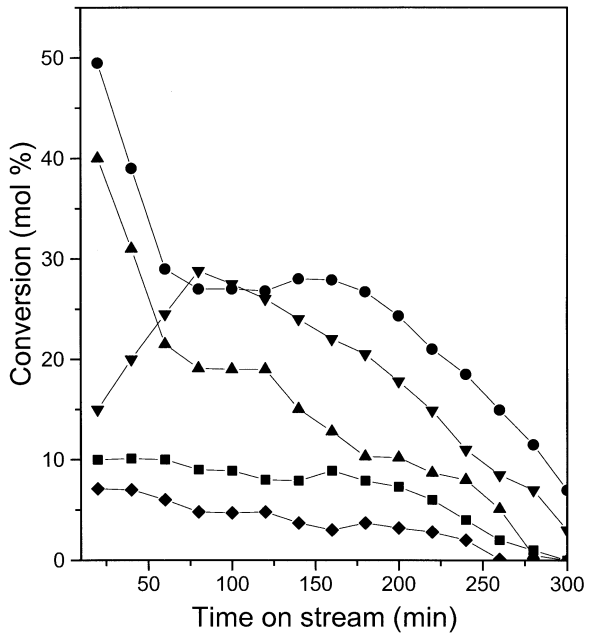

Figure 4. Conversion *versus* time on stream in *n*-butane isomerization at 245 kPa of pressure. (■) ZAS-10.7; (●) ZANS-10.7; (▲) ZANS-11.6; (▼) ZANS-12.5; (◆) ZANS-13.4.

that dehydrogenated intermediates adsorb strongly on the catalyst surface, thus leading to a rapid deactivation. Increasing the sulfate content of nickel–alumina ZrO_2 showed a detrimental effect for *n*-butane conversion (table 3). Higher sulfate contents seemed also to destabilize tetragonal ZrO_2 (table 2).

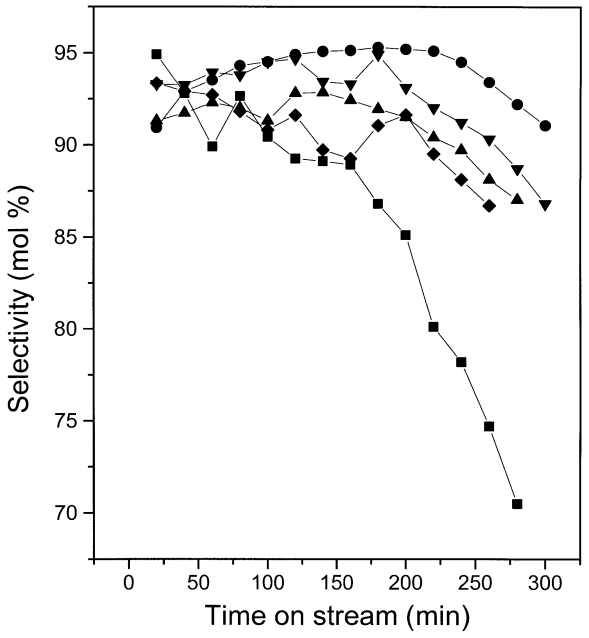

Figure 5. Selectivity to isobutane *versus* time on stream in *n*-butane isomerization reaction at 245 kPa of pressure. (■) ZAS-10.7; (●) ZANS-10.7; (▲) ZANS-11.6; (▼) ZANS-12.5; (◆) ZANS-13.4.

4. Discussion

The isomerization of *n*-butane has been proposed to proceed through a bimolecular mechanism [8,18,19]. According to this mechanism, a molecule of *n*-butane is dehydrogenated, producing an olefin that further reacts with an adsorbed carbocation on an acid center. The dimer thus formed follows transposition reactions and beta scission.

According to our results, the intrinsic catalytic activity seemed to be related to both the tetragonal phase of zirconia and to the acidity of the catalyst. The incorporation of a metal having redox properties to sulfated zirconia showed no changes in acidity but greatly increased the catalytic activity in isomerization reactions [20,21]. This has been put forward with nickel-sulfated zirconia [10,22,23]. The nickel probably incorporates into the zirconia lattice, thus stabilizing the tetragonal phase of zirconia. It seems that the electronic interaction between Zr–O–Ni bonds at the surface of tetragonal ZrO_2 inhibits the development of acidic properties, although it also increases the activity for isomerization.

In contrast, our samples showed that the acid site density strongly increased upon nickel addition, thus suggesting that the interaction between sulfate groups and nickel oxide generated both oxidizing and acid sites. Tetragonal zirconia seemed to be promoted by alumina, while nickel would increase acidity. It has already been reported that alumina showed a stabilizing effect on tetragonal zirconia [24]. In our samples, alumina addition led to a better dispersion of nickel as nickel oxide on the catalyst surface, inhibiting strong interaction between nickel and zirconia lattice [22]. The increase in catalytic activity with nickel addition would be consistent with the bimolecular mechanism. Nickel would accelerate *n*-butane dehydrogenation, thus producing olefins that react further with adsorbed carbocations produced on the acid sites.

Increasing the sulfate content from 10.7 to 12.5 wt% in our catalysts showed no major effect on *n*-butane conversion. Higher amounts of sulfate had a detrimental effect on the catalytic activity, as shown with sample ZANS-13.4. This could be associated with the relative content of tetragonal ZrO_2 that decreased dramatically (table 3). Farcasiu *et al.* [14] showed that when the coverage of sulfate groups were too high the transformation of the tetragonal to monoclinic phase in zirconia occurred.

Similar trends in intrinsic activity of the catalysts were observed independently of the reaction pressure (figure 6). At 245 kPa the catalytic activity was higher compared to runs conducted at atmospheric pressure (78 kPa). This difference could be attributed to the increase in *n*-butane concentration at the surface of the catalyst, thus enhancing the local concentration of olefins near the acid sites. At higher pressure the concentration of olefins and paraffins at the catalyst surface increased, favoring the oligomerization rate as well. The

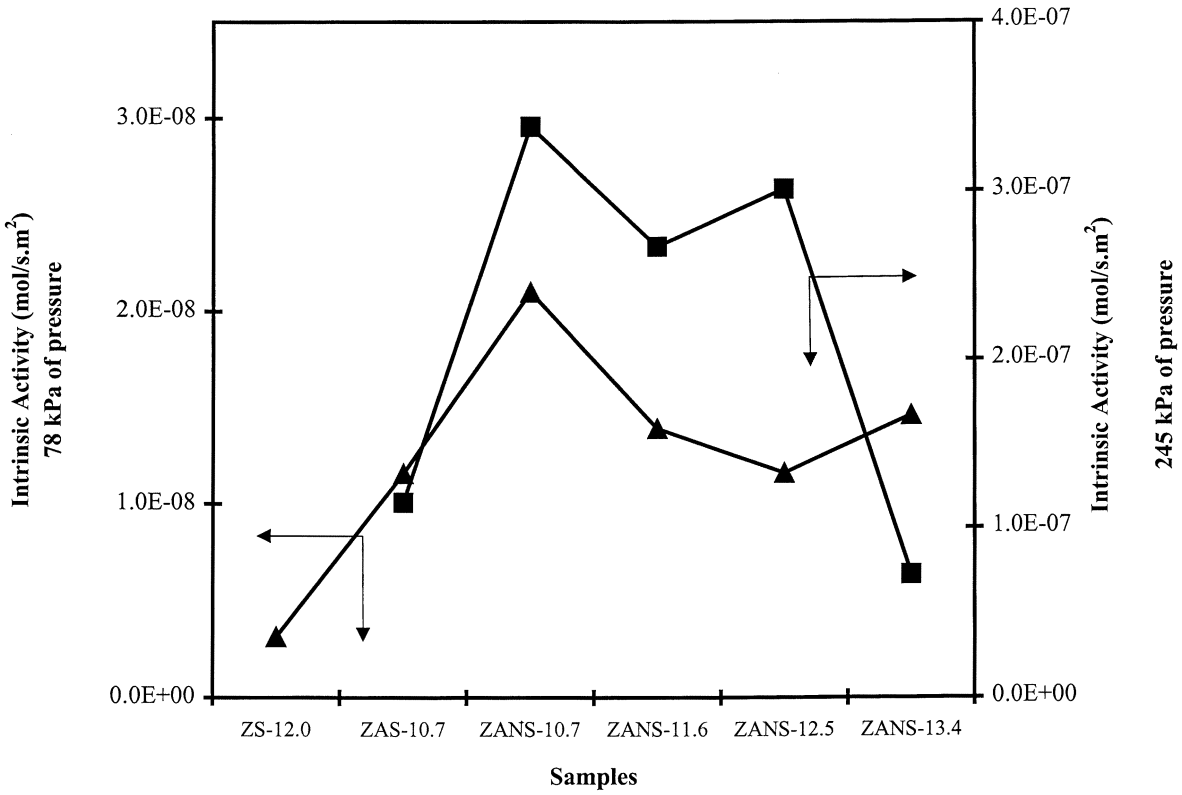

Figure 6. Intrinsic activity during *n*-butane isomerization reaction at atmospheric (■) (78 kPa) and (▲) 245 kPa pressures.

fact that no induction period was observed at higher pressure supported this mechanism. Since coke formation is related to the surface concentration of olefins [23], a higher deactivation rate was observed.

5. Conclusions

Tetragonal and monoclinic ZrO_2 were obtained, and the relative content varied depending on the presence of nickel, alumina and the degree of sulfation. Alumina stabilizes the tetragonal phase, leading to a better dispersion of the nickel in the form of nickel oxide at the surface of a catalyst, which increases the acid site density and the catalytic activity, through an increase of the dehydrogenation rate, which is the determining step in the bimolecular mechanism that operates during *n*-butane isomerization over sulfated zirconia promoted with transition metals.

The catalytic activity for *n*-butane isomerization greatly depended on the pressure. The effect of the pressure was to increase the hydrocarbon concentration at the catalyst surface, which at the same time causes an enhancement of the olefin concentration by an increase in the dehydrogenation and oligomerization rates.

Catalytic activity strongly increased the nickel–alumina samples, with sulfate content less than 13 wt%. The catalytic activity was explained by the interaction between sulfate groups and nickel oxide which generate both oxidizing and acidic sites. However, the existence of a higher concentration of tetragonal phase is also necessary.

Acknowledgments

This work was financially supported via Grant IMP-D.01234.

References

[1] P.J. Kuchar, J.C. Bricker, M.E. Reno and R.S. Haisman, Fuel Processing Technol. 35 (1993) 183.
[2] C. Monterra, G. Cerrato, C. Emanuel and V. Bolis, J. Catal. 142 (1993) 349.
[3] T.K. Cung, F.C. Lange and B. Gates, J. Catal. 159 (1996) 99.
[4] A.S. Zarcalis, F.C. Lange and B. Gates, J. Catal. 159 (1996) 1.
[5] C.R.Vera, J.C. Yori and J.M. Parera, Appl. Catal. A 167 (1998) 75.
[6] R. Srinivasan and A. Robert, J. Catal. 153 (1995) 123.
[7] J.M. Parera, Catal. Today 15 (1992) 481.
[8] J.E. Tabora and R.J. Davis, J. Am. Chem. Soc. 118 (1996) 12240.
[9] Y. Xia, W. Hua and Z. Gao, Appl. Catal. A 185 (1999) 293.
[10] M. Pérez, H. Armendariz, J.A. Toledo, A. Vazquéz, J. Navarrete, A. Montoya and A. García, J. Mol. Catal. 149 (1999) 169.
[11] J. Rodriguez-Carbajal, Laboratoire Leon Brillouin (CEA-CNRS), France.
[12] M.A. Cortes-Jacome, J.A. Toledo Antonio, H. Armendariz, I. Hernandez and X. Bokhimi, J. Solid. State. Chem. 2002, in press.
[13] X. Bokhimi, A. Morales, O. Novaro, M. Portilla, T. López, F. Txompantzi and R. Gómez, J. Solid State Chem. 135 (1998) 28.

[14] D. Farcasiu, J.Q. Li and S. Cameron, Appl. Catal. A 154 (1997) 173.
[15] R. Comelli, C. Vera and J. Parera, J. Catal. 151 (1995) 96.
[16] R. Keogh, D. Sparks and B. Davis, Stud. Surf. Sci. Catal. 88 (1994) 647.
[17] J.C. Yori, J. Luy and J. Parera, Appl. Catal. A 46 (1989) 103.
[18] V. Adeeva, G.D. Lei and W.M.H. Sachtler, Appl. Catal. A 118 (1994) LII.
[19] J.C. Yori and J.M. Parera, Appl. Catal. A 147 (1996) 145.
[20] C.Y. Hsu, C.R. Heimbuch, C.T. Armes and B.C. Gates, J. Chem. Soc. Chem. Commun. (1992) 1645.
[21] V. Adeeva, J.W. de Hann, J. Jänchen, G.D. Lei, V. Shünemann, L.J.M. van de Ven, W.M.H. Sachtler and R.A. Van Santen, J. Catal. 151 (1995) 364.
[22] M.A. Coelho, D.E. Resasco, E.C. Sikabwe and R.L. White, Catal. Lett. 32 (1995) 253.
[23] R.S. Drago and N. Kob, J. Phys. Chem. B 101 (1997) 3360.
[24] P. Canton, R. Olindo, F. Pinna, G. Strukul, P. Riello, M. Meneghetti, G. Cerrato, C. Morterra and A. Benedetti, Chem. Mater. 13 (2001) 1634.
[25] H. Armendáriz, A. Guzmán, J.A. Toledo, M.E. Llanos, A. Vázquez and G. Aguilar Ríos, Appl. Catal. A 211 (2001) 69.